

# Silyl derivatives of ferrocene with pending indenyl or fluorenyl substituents at silicon

Max Herberhold\*, Anahid Ayazi, Wolfgang Milius, Bernd Wrackmeyer\*

Laboratorium für Anorganische Chemie der Universität Bayreuth, Postfach 101251, D-95440 Bayreuth, Germany

Received 22 January 2002; received in revised form 2 April 2002; accepted 25 April 2002

Dedicated to Professor Gottfried Huttner on the occasion of his 65th birthday

## Abstract

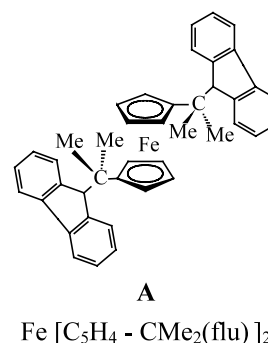
The reactions of chlorosilyl-substituted ferrocenes with indenyl lithium and fluorenyl lithium have been used to synthesise new ferrocene derivatives in which 1-indenyl (ind) or 9-fluorenyl (flu) substituents are connected with the ferrocene sandwich through a silicon bridge. In addition to the monosubstituted indenyl-silyl- and fluorenyl-silyl-ferrocenes  $\text{Fc-SiMe}_2(\text{ind})$  (**1a**),  $\text{Fc-SiMe}_2(\text{flu})$  (**1b**),  $\text{Fc-SiMe}(\text{Ph})(\text{flu})$  (**2b**),  $\text{Fc-SiMe}(\text{flu})_2$  (**3b**) and  $\text{Fc-SiCl}(\text{flu})_2$  (**4b**), the 1,1'-disubstituted ferrocenes  $\text{fc}[\text{SiMe}_2(\text{ind})]_2$  (**5a**) and  $\text{fc}[\text{SiMe}_2(\text{flu})]_2$  (**5b**) as well as the 1-sila-[1]ferrocenophanes  $\text{fc}[\text{SiMe}(\text{ind})]$  (**6a**) and  $\text{fc}[\text{SiMe}(\text{flu})]$  (**6b**) were included in this study. The products were characterised in solution by  $^1\text{H}$ -,  $^{13}\text{C}$ - and  $^{29}\text{Si}$ -NMR spectroscopy and by mass spectrometry. The molecular structures of the di(fluorenyl)silyl ferrocenes **3b** and **4b** and of the 1-sila-[1]ferrocenophanes **6a** and **6b** were determined by single crystal X-ray crystallography. © 2002 Elsevier Science B.V. All rights reserved.

**Keywords:** Ferrocenes; Silanes; Indenyl; Fluorenyl; X-ray

## 1. Introduction

The synthesis of ferrocenes bearing planar substituents such as cyclopentadienyl (Cp), indenyl (ind) or fluorenyl (flu) in the side-chain has attracted some interest because these groups are able to act as ligand functionalities for the construction of di- and trinuclear complexes (which may incorporate different metals). In the present study the indenyl and fluorenyl derivatives are preferentially investigated, because the large indenyl and fluorenyl substituents were found to reduce the number of isomers which are formed, and because they are more flexible compared to cyclopentadienyl with respect to ring slippage in additional complexations. Both 1,1'-bis(dimethylindenylmethyl)ferrocene,  $\text{Fe}[\text{C}_5\text{H}_4\text{-CMe}_2(\text{ind})]_2$  [**1**], and 1,1'-bis(dimethylfluorenylmethyl)ferrocene,  $\text{Fe}[\text{C}_5\text{H}_4\text{-CMe}_2(\text{flu})]_2$  (**A**) [**2,3**], have

been described. According to the X-ray structure determination of the fluorenyl compound **A** [**3**], the conformational arrangement of the two  $\eta^5$ -cyclopentadienyl rings [**4**] in the crystal is  $\tau = 171.3^\circ$ , i.e. the molecule approaches the staggered conformation ( $\tau = 180^\circ$ ) although it is not centrosymmetric [**3**].



A series of ferrocenyl-indenyl compounds without or with spacer ( $-\text{CH}_2-$ ,  $-\text{C}\equiv\text{C}-$ ,  $-\text{C}_6\text{H}_4-$ ) between the two groups and their CpFe adducts have also been described [**31**].

\* Corresponding authors. Tel.: +49-921-552540; fax: +49-921-552157

E-mail addresses: max.herberhold@uni-bayreuth.de (M. Herberhold), b.wrack@uni-bayreuth.de (B. Wrackmeyer).

We now report on some silyl-substituted ferrocene derivatives in which the 1-indenyl or 9-fluorenyl substituents are attached to silicon.

## 2. Results and discussion

### 2.1. Synthesis

The lithiation of ferrocene ( $\text{FeCp}_2$ ,  $\text{FcH}$ ) can be conducted selectively to give either monolithio-ferrocene,  $\text{FcLi}$  [5] (using *t*-BuLi in THF solution), or 1,1'-dilithio-ferrocene,  $\text{fcLi}_2(\text{tmeda})_n$  ( $n = 1$  or 2) [6] (using *n*-BuLi in hexane in the presence of tetramethylethylenediamine). Subsequent reactions of the lithiated ferrocenes with methylchlorosilanes lead to the chlorosilyl-substituted ferrocene derivatives **1–6** (Schemes 1 and 2) which had been characterised previously [7–12].

Starting from monolithio-ferrocene, the monosubstituted ferrocenes **1–4** were prepared. Starting from 1,1'-dilithio-ferrocene, either 1,1'-disilyl-substituted ferrocenes (such as **5**) or 1-sila-[1]ferrocenophanes (such as **6**) became accessible.

The reactions of the chlorosilyl-substituted ferrocenes **1–5** and the 1-sila-[1]ferrocenophane **6** with indenyl- and fluorenyl lithium afforded the desired 1-indenyl (**a**) and 9-fluorenyl (**b**) derivatives **1a,b**, **2b–4b**, **5a,b** and **6a,b** (Scheme 3) under concomitant formation of LiCl.

Attempts to prepare the 1-indenyl analogues of **2b–4b** were not successful so far. Although two 9-fluorenyl substituents at silicon are tolerated (**3b** and **4b**), the last chloro substituent in **4b** could not be displaced for a third fluorenyl group.

All indenyl (**1a**, **5a**, **6a**) and fluorenyl (**1b–6b**) complexes showed the molecular ion  $[\text{M}^+]$  in the electron-impact mass spectra. The peak of highest intensity (100%) always corresponds to the fragment ion generated from  $[\text{M}^+]$  by loss of one indenyl or fluorenyl group.

### 2.2. X-ray studies

The molecular structures of di(9-fluorenyl)methylsilyl- and di(9-fluorenyl)chlorosilyl-ferrocene (**3b** and **4b**, respectively, Fig. 1) and of the two 1-sila-[1]ferrocenophanes **6a** and **6b** (Fig. 2) were determined by X-ray crystallography; selected bond lengths and angles are collected in Tables 1 and 2.

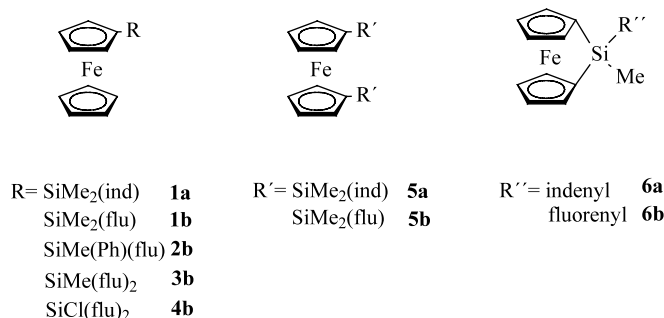
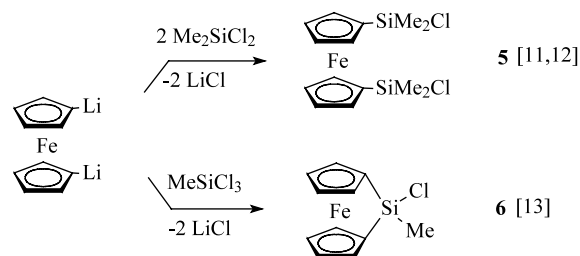
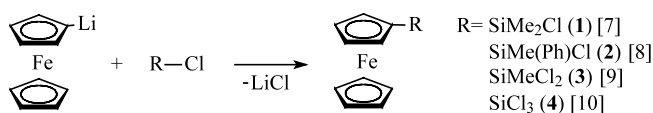


Table 1 contains a comparison of the bond lengths and angles of the three fluorenyl complexes **3b**, **4b** and **6b**. The two di(9-fluorenyl)-substituted silanes,  $\text{Fc-SiMe}(\text{flu})_2$  (**3b**) and  $\text{Fc-SiCl}(\text{flu})_2$  (**4b**), both form triclinic crystals with space group  $P\bar{1}$ , they are crowded molecules like di(9-fluorenyl)dimethylsilane,  $\text{SiMe}_2(\text{flu})_2$  [14]. The two cyclopentadienyl rings of the ferrocene unit are nearly parallel (tilt angle  $\alpha = 2.6$  and  $0.7^\circ$  in **3b** and **4b**, respectively, cf. Table 3) and adopt an almost eclipsed conformation (with twist angles of 2.5 and  $1.4^\circ$ , respectively, cf. Table 3). As expected, the dihedral angles between the plane of the substituted cyclopentadienyl ring and the respective fluorenyl system differ considerably: in the case of **3b**, the angles are  $85.0$  and  $48.3^\circ$ , while in the case of **4b** the angles are  $86.5$  and  $112.8^\circ$ , i.e. in both complexes one of the two fluorenyl substituents is arranged in an almost orthogonal position relative to the ferrocene cyclopentadienyl rings. The dihedral angles between the two fluorenyl planes are  $117.6^\circ$  in **3b** and  $122.3^\circ$  in **4b**; the corresponding angles are  $80.1$  and  $96.8^\circ$  in the two non-identical molecules of  $\text{SiMe}_2(\text{flu})_2$  [14] which are present in the orthorhombic crystal.

The bond angles around silicon are found within the range expected for a basically tetrahedral geometry ( $109.5^\circ$ ), i.e. between  $105$  and  $115^\circ$  in **3b** and between  $103$  and  $116^\circ$  in **4b**, cf.  $105$ – $112^\circ$  in  $\text{SiMe}_2(\text{flu})_2$  [14]. The bond vectors from Si to the fluorenyl substituents ( $\text{Si-C}(9)$ ) and  $\text{Si-C}(9')$ ) include an angle with the respective fluorenyl plane which is  $137.2$  (flu) and  $146.6^\circ$  (flu') in **3b** as well as  $145.4$  and  $131.3^\circ$  in **4b**. Therefore, the valence

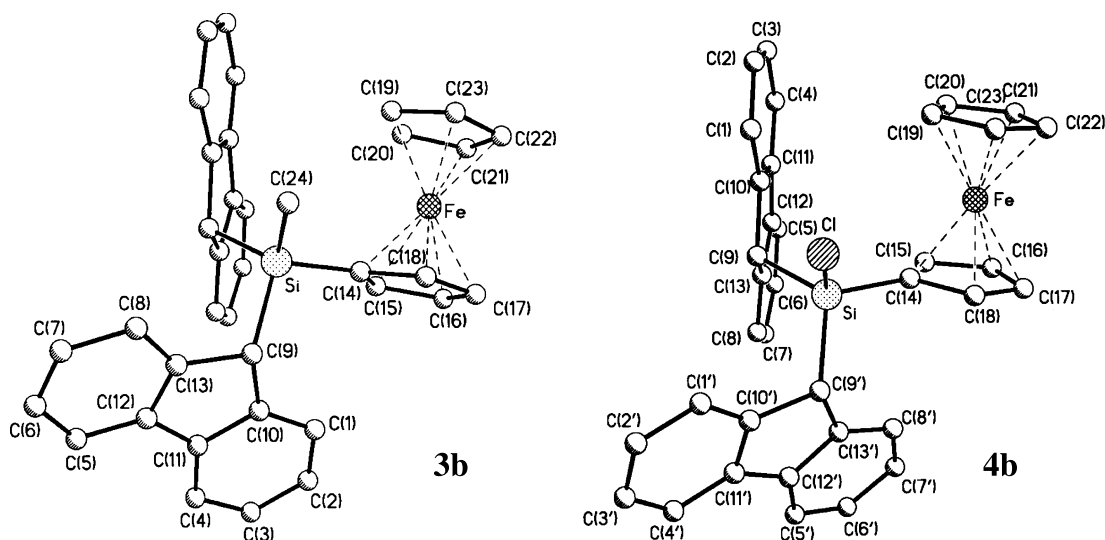


Fig. 1. Molecular structures of  $\text{Fc-SiMe}(\text{flu})_2$  (**3b**) and  $\text{Fc-SiCl}(\text{flu})_2$  (**4b**).

angle  $\text{C}(9)\text{-Si-C}(9')$  is only slightly larger than the ideal tetrahedral angle of  $109.5^\circ$ . The tetrahedral coordination sphere of silicon in ferrocenyl-substituted silanes has been confirmed in many cases, e.g. in  $\text{SiFc}_4$  [15],  $\text{Si}(\text{Fc})_2(\text{OH})_2$  [16],  $\text{Fc-SiMe}_2\text{SiMe}_2\text{-Fc}$  [17] and  $\text{fc}[\text{Si-Me}_2\text{Fc}]_2$  [19].

In **3b** and **4b** the bulky di(9-fluorenyl)silyl substituents (R) are slightly bent outwards from their respective cyclopentadienyl planes, away from iron (cf. angles  $\beta$  in Table 3). The reverse situation is characteristic of 1-sila-[1]ferrocenophanes [18,19a], including **6a** and **6b**. The 1-indenyl substituent in **6a** (see Table 2) apparently tolerates smaller deviation angles ( $\beta = 37.0^\circ$  av) than the larger 9-fluorenyl substituent in **6b** ( $\beta = 38.2^\circ$  av); i.e. the non-bonding distance  $\text{Fe}\cdots\text{Si}$  is slightly longer in

**6a** (272.5 pm) than in **6b** (269.2 pm). Similar non-bonding  $\text{Fe}\cdots\text{Si}$  distances have been found in  $\text{fc}[\text{SiMe}_2]$  (269.0 pm [20]) and  $\text{fc}[\text{SiMe}(\text{Fc})]$  (270.8 pm [19]), the shortest distance was reported for the case of  $\text{fc}[\text{SiPh}_2]$  (268 pm [21]).

It is not surprising that the ferrocenophane unit in both **6a** and **6b** is a highly symmetrical building block, the cyclopentadienyl rings are arranged exactly eclipsic ( $\tau = 0$ , cf. Table 3), and the Si atom is found in the plane which is determined by the Fe atom and the midpoints of the cyclopentadienyl rings. It is remarkable, however, that the planes of the indenyl and fluorenyl substituents, respectively, are nearly perpendicular to the plane containing Fe, Si and the methyl carbon and bisecting the ferrocenophane unit,  $[\text{Fe}(\text{C}_5\text{H}_4)_2\text{Si}]$ , the dihedral

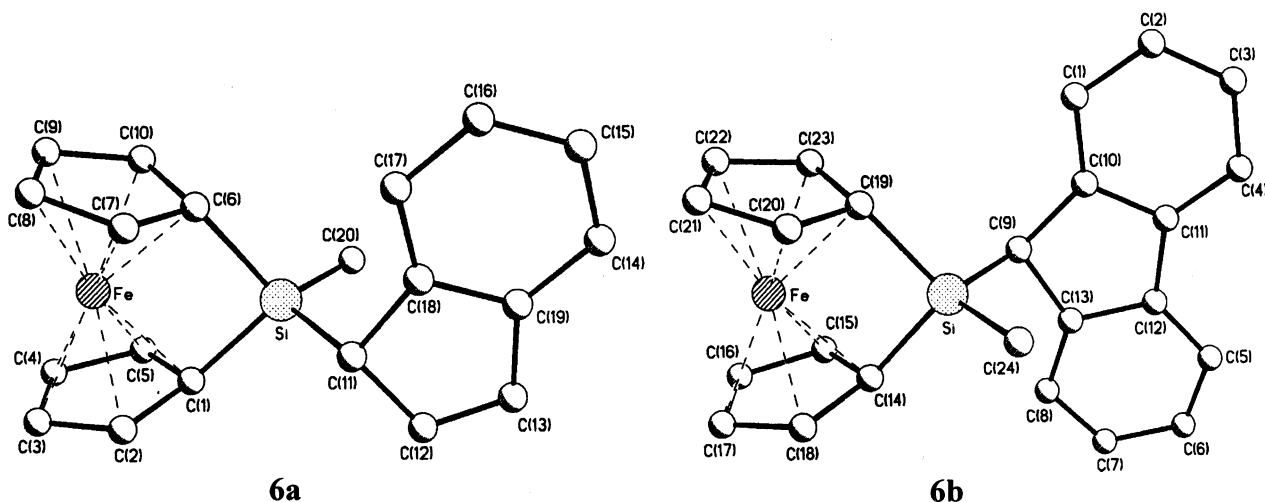


Fig. 2. Molecular structures of  $\text{fc}[\text{SiMe}(\text{ind})]$  (**6a**) and  $\text{fc}[\text{SiMe}(\text{flu})]$  (**6b**).

Table 1  
Selected bond lengths (pm) and bond angles (°) in the fluorenyl complexes **3b**, **4b** and **6b**

Complex	Fc–SiMe(flu) <sub>2</sub> ( <b>3b</b> )	Fc–SiCl(flu) <sub>2</sub> ( <b>4b</b> )	fc[SiMe(flu)] ( <b>6b</b> )
<i>Bond lengths (Å)</i>			
Si–C(9)	192.4(4)	189.1(2)	189.1(5)
Si–C(9')	191.0(5)	189.1(2)	
Si–C(14)	184.6(5)	183.6(2)	187.9(5)
Si–C(19)			187.8(5)
Si–C(24)	187.3(5)		184.3(6)
Si–Cl		206.91(10)	
Fe–C(14)	205.4(4)	204.7(2)	202.2(5)
Fe–C(15)	203.4(4)	204.2(2)	202.0(5)
Fe–C(16)	203.7(5)	205.4(2)	207.2(6)
Fe–C(17)	206.6(5)	205.3(2)	206.9(6)
Fe–C(18)	204.2(4)	203.2(2)	202.2(6)
Fe–C(19)	205.5(5)	204.1(3)	200.7(5)
Fe–C(20)	203.1(5)	203.4(3)	202.9(5)
Fe–C(21)	204.1(5)	204.0(3)	206.7(5)
Fe–C(22)	204.2(5)	204.1(3)	206.7(6)
Fe–C(23)	204.0(5)	204.7(3)	203.0(5)
Fe...Si			269.2
C(1)–C(2)	137.8(7)	139.6(5)	138.8(9)
C(1)–C(10)	138.6(7)	135.8(4)	138.9(8)
C(2)–C(3)	135.7(10)	137.9(6)	138.1(10)
C(3)–C(4)	137.3(10)	137.0(5)	136.9(9)
C(4)–C(11)	141.7(8)	138.6(4)	138.7(8)
C(5)–C(6)	136.4(12)	137.5(4)	135.3(10)
C(5)–C(12)	139.8(8)	139.4(4)	139.6(8)
C(6)–C(7)	135.4(13)	135.7(5)	138.3(11)
C(7)–C(8)	142.7(11)	139.4(4)	139.0(9)
C(8)–C(13)	138.3(8)	137.8(4)	138.0(8)
C(9)–C(10)	151.0(6)	151.4(3)	150.5(7)
C(9)–C(13)	151.4(7)	152.2(3)	151.1(7)
C(10)–C(11)	140.3(7)	140.1(4)	140.3(7)
C(11)–C(12)	142.9(8)	146.1(4)	145.1(8)
C(12)–C(13)	139.9(8)	138.9(3)	140.4(8)
<i>Bond angles (°)</i>			
C(9)–Si–C(14)	105.50(19)	115.32(11)	109.9(2)
C(9')–Si–C(14)	114.8(2)	106.98(11)	
C(9)–Si–C(24)	106.4(2)		111.2(3)
C(9')–Si–C(24)	111.6(2)		
C(9)–Si–C(9')	110.2(2)	114.69(11)	
C(9)–Si–C(19)			111.5(2)
C(9)–Si–Fe			122.49(17)
C(9)–Si–Cl		107.68(8)	
C(9')–Si–Cl		103.04(8)	
C(14)–Si–Cl		108.28(8)	
C(14)–Si–C(19)			96.8(2)
C(14)–Si–C(24)	107.9(2)		114.3(3)
C(19)–Si–C(24)			112.4(3)
Si–C(9)–C(10)	117.1(3)	113.32(16)	111.5(3)
Si–C(9)–C(13)	116.5(3)	112.23(16)	110.0(4)
Si–C(14)–C(15)	132.0(3)	129.05(17)	119.0(4)
Si–C(14)–C(18)	122.2(3)	124.00(19)	118.7(4)
Si–C(14)–Fe			87.2(2)
Si–C(19)–Fe			87.7(2)

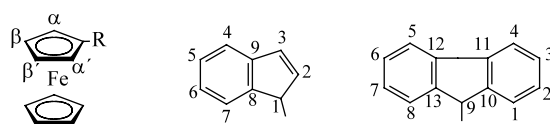
Table 2  
Selected bond lengths (pm) and bond angles (°) in 1-methyl-1-indenyl-sila-[1]ferrocenophane, fc[SiMe(ind)] (**6a**)

Bond lengths (Å)		Bond angles (°)	
Si–C(1)	189.5(4)	C(1)–Si–C(6)	95.34(18)
Si–C(6)	188.3(4)	C(1)–Si–C(11)	111.34(18)
Si–C(11)	187.8(4)	C(1)–Si–C(20)	112.1(2)
Si–C(20)	184.9(5)	C(6)–Si–C(11)	110.28(19)
Si...Fe	272.5	C(6)–Si–C(20)	114.5(2)
		C(11)–Si–C(20)	112.2(2)
Fe–C(1)	200.9(4)	C(11)–Si–Fe	122.67(14)
Fe–C(2)	202.9(4)	C(20)–Si–Fe	125.10(18)
Fe–C(3)	208.0(4)		
Fe–C(4)	209.0(4)	Si–C(1)–C(2)	120.8(3)
Fe–C(5)	202.8(5)	Si–C(1)–C(5)	118.3(3)
Fe–C(6)	202.1(4)	Si–C(11)–C(12)	112.3(3)
Fe–C(7)	203.2(4)	Si–C(11)–C(18)	111.7(3)
Fe–C(8)	208.1(4)	Si–Fe–C(1)	44.05(12)
Fe–C(9)	207.9(4)	Si–Fe–C(6)	43.71(12)
Fe–C(10)	203.6(4)		
C(11)–C(12)	150.5(6)	C(12)–C(11)–C(18)	101.5(3)
C(11)–C(18)	150.7(5)	C(11)–C(12)–C(13)	111.3(4)
C(12)–C(13)	132.8(6)	C(12)–C(13)–C(19)	110.1(4)
C(13)–C(19)	146.5(7)	C(11)–C(18)–C(19)	109.9(4)
C(14)–C(15)	138.8(7)	C(13)–C(19)–C(18)	107.0(4)
C(14)–C(19)	139.6(6)		
C(15)–C(16)	137.6(7)		
C(16)–C(17)	138.7(6)		
C(17)–C(18)	139.0(6)		
C(18)–C(19)	140.0(6)		

indenyl plane is 146.9° in **6a**, the corresponding angle between the Si–C(9) vector (189.1(5) pm) and the fluorenyl plane 147.2° in **6b**.

The angles at the pseudo-tetrahedral silicon centre are comparable in **6a** and **6b**. While the intra-ferrocenophane angles are small (C(1)–Si–C(6) = 95.34(18)° in **6a** and C(14)–Si–C(19) = 96.8(2)° in **6b**), all other angles C–Si–C are found between 110 and 115°, somewhat larger than the ideal tetrahedral angle of 109.5°.

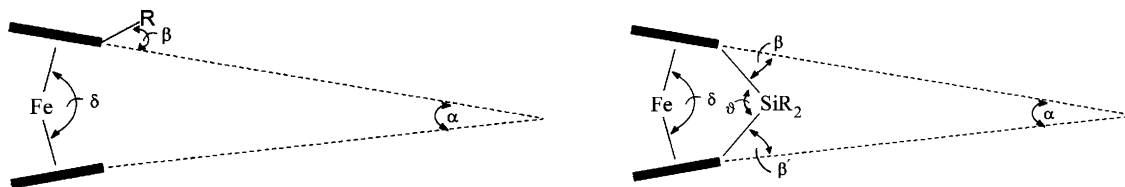
The dihedral angles ( $\alpha$ ) between the two cyclopentadienyl ring planes (Table 3) are found to be 21.2° in **6a** and 20.2° in **6b**, which are typical values for 1-sila-[1]ferrocenophanes [15,18]. Comparable inclination angles  $\alpha$  have been observed for fc[SiCl<sub>2</sub>] (19.2(4)° [13]), fc[SiPh<sub>2</sub>] (19.2° [21]), fc[SiMe<sub>2</sub>] (20.8(5)° [15,20]) and fc[SiMe(Fe)] (21.3° [19a]). The inclination of the two cyclopentadienyl ring planes (angle  $\alpha$ ) can also be characterised by the angle  $\delta$  at the iron atom between

CpFe(C<sub>5</sub>H<sub>4</sub>) (Fc)C<sub>9</sub>H<sub>7</sub> (ind)C<sub>13</sub>H<sub>9</sub> (flu)

Scheme 4.

angles being 95.0 (**6a**) and 87.1° (**6b**), respectively. The angle between the Si–C(11) vector (187.8(4) pm) and the

Table 3  
Geometry of the ferrocene unit in complexes **3b**, **4b**, **6a** and **6b**



Complex	<b>3b</b>	<b>4b</b>	<b>6a</b>	<b>6b</b>
$\alpha$ [°] <sup>a</sup>	2.6	0.7	21.2	20.2
$\beta$ [°] <sup>b</sup>	9.8 (outwards)	11.8 (outwards)	36.8	38.4
$\delta$ [°] <sup>c</sup>	177.6	178.9	37.2	38.0
$\tau$ [°] <sup>d</sup>	2.5	1.4	164.2	164.6
$\vartheta$ [°] <sup>e</sup>			0	0
			95.34(18)	96.8(2)

<sup>a</sup> Inclination of the two cyclopentadienyl ring planes.

<sup>b</sup> Deviation of the silyl substituent from its cyclopentadienyl plane.

<sup>c</sup> Angle at iron between the two centers of the cyclopentadienyl rings.

<sup>d</sup> Conformational deviation of the cyclopentadienyl rings from the eclipsed form ( $\tau = 0$ ).

<sup>e</sup> Angle at silicon within the [1]ferrocenophane unit.

Table 4  
<sup>1</sup>H- and <sup>29</sup>Si-NMR data of the starting complexes **1–6** and fluorenyl derivatives **1b–6b** in CDCl<sub>3</sub>

No. Complex	<sup>1</sup> H-NMR <sup>a,b</sup>				<sup>29</sup> Si-NMR						
	Ferrocene		Fluorenyl								
	Cp	H <sup>α</sup>	H <sup>β</sup>	CH <sub>3</sub> (Si)	H <sup>1</sup> ,H <sup>8</sup>	H <sup>2</sup> ,H <sup>7</sup>	H <sup>3</sup> ,H <sup>6</sup>	H <sup>4</sup> ,H <sup>5</sup>	H <sup>9</sup>		
 [25, 27]					7.55	7.28	7.38	7.84	3.87		
<b>1</b> Fc-SiMe <sub>2</sub> Cl	4.16	4.21	4.42	0.65						22.7	
<b>1b</b> Fc-SiMe <sub>2</sub> (flu)	4.04	3.93	4.36	0.12		7.34-7.18		7.83	3.86	0.6	
								7.80			
<b>2</b> Fc-SiMe(Ph)Cl	4.16	4.30 or 4.44		0.92		(Phenyl 7.70-7.67(2); 7.43-7.40 (3))				13.5	
		4.23									
<b>2b</b> Fc-SiMe(Ph)(flu)	3.74	4.21	4.41	0.08		7.33-6.88		7.84	3.64	-4.7	
		4.15	4.31					7.81			
						(Phenyl 7.66(2); 7.47(3))					
<b>3</b> Fc-SiMeCl <sub>2</sub>	4.23	4.32	4.48	0.98						22.3	
<b>3b</b> Fc-SiMe(flu) <sub>2</sub>	3.46	4.14	3.22	0.21		7.41-7.05		7.93	4.16	2.3	
								7.90			
<b>4</b> Fc-SiCl <sub>3</sub>	4.27	4.41 or 4.57								2.1	
<b>4b</b> Fc-SiCl(flu) <sub>2</sub>	3.57	4.27	3.39			7.11	7.22	7.36	7.86	3.91	18.3
						6.86					
<b>5</b> fc[SiMe <sub>2</sub> Cl] <sub>2</sub>		4.22	4.42	0.64						23.2	
<b>5b</b> fc[SiMe <sub>2</sub> (flu)] <sub>2</sub>		3.86	4.21	0.10		7.36-7.22		7.84	3.84	0.8	
								7.81			
<b>6</b> fc[SiMeCl]		4.27	4.60	0.85						5.6	
		4.07	4.55								
<b>6b</b> fc[SiMe(flu)]		4.56	4.66	-0.45		7.80	7.34	7.41	7.95	4.31	-1.4
		4.07	4.56			7.77	7.31	7.38	7.92		

<sup>a</sup>Assigned according to NOE and 2D <sup>13</sup>C–<sup>1</sup>H HETCOR experiments for **1b**, **3b** and **6b**. <sup>b</sup>Except of the <sup>1</sup>H(SiMe) and <sup>1</sup>H(Cp) signals all other signals appear as multiplets which were not analysed.

Table 5  
 $^{13}\text{C}$ -NMR data of the starting complexes **1–6** and fluorenyl derivatives **1b–6b** in  $\text{CDCl}_3$

No.	Complex	Ferrocene				Fluorenyl							
		Cp	$\text{C}^i$	$\text{C}^\alpha$	$\text{C}^\beta$	$\text{CH}_3(\text{Si})$	$\text{C}^1, \text{C}^8$	$\text{C}^2, \text{C}^7$	$\text{C}^3, \text{C}^6$	$\text{C}^4, \text{C}^5$	$\text{C}^9$	$\text{C}^{10}, \text{C}^{13}$	$\text{C}^{11}, \text{C}^{12}$
cf.	$\text{SiMe}_3(\text{flu})$ [26]					–2.5	124.6	126.6	125.95	120.6	43.3	146.4	141.3
<b>1</b>	$\text{Fc-SiMe}_2\text{Cl}$	68.0	68.3	72.9 <sup>a</sup>	71.7	2.9							
<b>1b</b>	$\text{Fc-SiMe}_2(\text{flu})$	68.17	68.24	73.7 <sup>a</sup>	70.9	–4.2	124.5	125.6	125.1	119.7	43.5	145.4	140.5
<b>2</b>	$\text{Fc-SiMe}(\text{Ph})\text{Cl}$ <sup>b</sup>	68.8	66.9	73.5	71.8	1.5							
				73.4	71.7								
<b>2b</b>	$\text{Fc-SiMe}(\text{Ph})(\text{flu})$ <sup>c</sup>	68.3	66.3	74.4	71.5	–7.8	124.9	125.8	125.3	119.7	42.0	145.0	140.7
				73.9	70.8		124.4 <sup>c</sup>	125.6	125.3	119.5		144.8	140.5
<b>3</b>	$\text{Fc-SiMeCl}_2$	69.3	66.0	73.0	or 72.3	6.5							
<b>3b</b>	$\text{Fc-SiMe}(\text{flu})_2$	68.1	65.5	70.7 <sup>a</sup>	73.9	–4.3	124.9	126.1	125.7	120.1	41.0	145.2	141.1
							124.9	125.9	125.6	119.8		144.9	140.8
<b>4</b>	$\text{Fc-SiCl}_3$	69.4	69.8	73.7	72.9								
<b>4b</b>	$\text{Fc-SiCl}(\text{flu})_2$	68.8	64.4	71.6 <sup>a</sup>	74.1		125.1	126.4	126.0	119.9	42.2	142.8	141.3
								126.3		119.8		142.7	141.1
<b>5</b>	$\text{fc}[\text{SiMe}_2\text{Cl}]_2$		69.3	73.3 <sup>a</sup>	72.5	2.9							
<b>5b</b>	$\text{fc}[\text{SiMe}_2(\text{flu})]_2$		69.1	73.8 <sup>a</sup>	71.6	–4.2	124.4	125.6	125.1	119.7	43.4	145.2	140.4
<b>6</b>	$\text{fc}[\text{SiMeCl}]$		33.5	75.7 <sup>a</sup>	78.6	0.4							
				73.6	78.3								
<b>6b</b>	$\text{fc}[\text{SiMe}(\text{flu})]$		36.7	75.3 <sup>a</sup>	71.6	–9.9	124.7	126.3	125.7	119.7	37.7	143.0	140.6
			33.6	75.2	77.5								

<sup>a</sup> Assignment to  $\text{C}^\alpha$  confirmed by NOE and/or 2D  $^{13}\text{C}$ – $^1\text{H}$  HETCOR experiments (see Section 2.3).

<sup>b</sup>  $^{13}\text{C}$ -NMR data of the phenyl substituent in **2**: 136.0 (*i*), 133.5 (*o*), 130.2 (*p*), 127.9 (*m*)<sup>d</sup>.

<sup>c</sup>  $^{13}\text{C}$ -NMR data of the phenyl substituent in **2b**: 136.8 (*i*), 134.3 (*o*), 129.4 (*p*), 127.8 (*m*)<sup>d</sup>.

<sup>d</sup>  $^{13}\text{C}$ -NMR data for  $\text{Ph-SiMe}_3$ : 140.1 (*i*), 133.4 (*o*), 128.9 (*p*), 127.8 (*m*) [25].

the two midpoints of the cyclopentadienyl rings (Table 3).

### 2.3. NMR spectra

The  $^1\text{H}$ -,  $^{13}\text{C}$ - and  $^{29}\text{Si}$ -NMR spectroscopic data of the new indenyl and fluorenyl complexes are compiled in the Tables 4–7. The following numbering scheme has been used for the ferrocene unit and for the indenyl and fluorenyl substituents (Scheme 4).

In the case of the fluorenyl substituents in the complexes **1b–6b**, the NMR numbering system corresponds to that used in the X-ray-determined molecular structures of the three fluorenyl derivatives **3b**, **4b** and **6b** (Figs. 1 and 2).

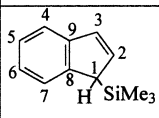
The  $^1\text{H}$ -NMR signals of the ferrocene sandwich units were assigned to the hydrogens in positions  $\alpha$  (close) and  $\beta$  (distant), relative to the substituent R, on the basis of 1D and 2D NOE experiments for the complexes **1b**, **3b**, **5b** and **6a,b**. For example, irradiation into the methyl absorption ( $\delta(^1\text{H})$  0.21) of  $\text{Fc-SiMe}(\text{flu})_2$  (**3b**) gives the NOE response for the pseudo-triplet at  $\delta$  4.19 which therefore corresponds to the  $\alpha$  protons. The number of assigned ferrocene  $^1\text{H}$ - and  $^{13}\text{C}$ -NMR signals in related complexes is limited in the literature, but the data reported for  $\text{fc}[\text{SiMe}_3]_2$  [22],  $\text{fc}[\text{SiMe}_2\text{Cl}]_2$  (**5**) [12], and for the stannyl-substituted series  $\text{fc}[\text{SnMe}_3]_2$ ,  $\text{fc}[\text{SnMe}_2\text{Cl}]_2$ ,  $\text{fc}[\text{SnMeCl}_2]_2$ ,  $\text{fc}[\text{SnCl}_3]_2$  [23] are fully consistent with the assignments given in the Tables 1–3.

For the assignment of the  $^{13}\text{C}$ -NMR signals to the cyclopentadienyl carbon atoms  $\text{C}^\alpha$  and  $\text{C}^\beta$ , 2D  $^{13}\text{C}$ – $^1\text{H}$  HETCOR experiments were used in several cases (**1/1b**, **3/3b**, **5/5b**, **6/6b**). The  $^{13}\text{C}$ -NMR signal for the quaternary ipso carbon atom,  $\text{C}^i$ , can easily be identified on the basis of its low intensity and ATP (attached proton test) experiments. The complexes **2** and **2b**, in which each silicon atom bears four different substituents, show four different signals for the  $^1\text{H}$  and  $^{13}\text{C}$  atoms in the positions  $\alpha$ ,  $\alpha'$  and  $\beta$ ,  $\beta'$ . A similar situation with four different cyclopentadienyl signals ( $\alpha$ ,  $\alpha'$ ,  $\beta$ ,  $\beta'$ ) is characteristic of the 1-sila-[1]ferrocenophanes **6**, **6a** and **6b**; two  $^{13}\text{C}^i$ -NMR signals are observed in **6a** and **6b** but not in the parent complex  $\text{fc}[\text{SiMeCl}]$  (**6**) ( $\delta(^{13}\text{C}^i)$  33.5). The chirality of the indenyl compounds,  $\text{Fc-SiMe}_2(\text{ind})$  (**1a**) and  $\text{fc}[\text{SiMe}_2(\text{ind})]_2$  (**5a**), can be deduced from the fact that **1a** possesses two and **5a** four methyl signals both in the  $^1\text{H}$  and  $^{13}\text{C}$  spectra (cf. Tables 6 and 7), whereas a single signal is observed in the spectra of the parent chlorosilanes  $\text{Fc-SiMe}_2\text{Cl}$  (**1**) and  $\text{fc}[\text{SiMe}_2\text{Cl}]_2$  (**5**) as well as in the corresponding fluorenyl compounds, **1b** and **5b**.

The chemical shifts  $\delta(^{29}\text{Si})$  change in the usual way [24] dependent on the substituent pattern. The influence of indenyl and fluorenyl groups on  $\delta(^{29}\text{Si})$  is very similar in the complexes **1a,b** and **5a,b**, whereas the  $^{29}\text{Si}$  nuclear shielding in the [1]ferrocenophane **6a** is slightly increased by 3.4 ppm with respect to the fluorenyl derivative **6b**, although the relevant structural para-



Table 6  
 $^1\text{H}$ - and  $^{29}\text{Si}$ -NMR data of the indenyl complexes **1a**, **5a** and **6a** in  $\text{CDCl}_3$

No. Complex	$^1\text{H}$ -NMR <sup>a</sup>							$^{29}\text{Si}$ -NMR	
	Ferrocene			$\text{CH}_3(\text{Si})$	Indenyl				
	Cp	$\text{H}^\alpha$	$\text{H}^\beta$			$\text{H}^1$	$\text{H}^2$	$\text{H}^3$	$\text{H}^4\text{-H}^7$
 (neat) [25,27]				0.24	3.32	6.49	6.79	7.2	
<b>1a</b> Fc-SiMe <sub>2</sub> (ind)	4.17	4.15	4.44	0.17	3.63dd <sup>b</sup>	6.68dd <sup>c</sup>	6.95ddd <sup>d</sup>	7.19-7.37	0.5
				0.22					
<b>5a</b> fc[SiMe <sub>2</sub> (ind)] <sub>2</sub>		4.01	4.29	0.10	3.50dd <sup>b</sup>	6.58dd <sup>c</sup>	6.87ddd <sup>d</sup>	7.08-7.44	-0.5
				0.11					
				0.12					
				0.13					
<b>6a</b> fc[SiMe(ind)]	4.20 <sup>e</sup>	4.62	-0.22		4.06	6.87dd <sup>c</sup>	7.10 ddd <sup>d</sup>	7.55-7.70	-4.8
	4.07	4.59						7.19-7.33	

<sup>a</sup>If not indicated otherwise all  $^1\text{H}$ -NMR signals are multiplets except of the  $^1\text{H}(\text{SiMe})$  and  $^1\text{H}(\text{Cp})$  signals. <sup>b</sup> $^3J(\text{H}^1, \text{H}^2) = 1.9$  Hz,  $^4J(\text{H}^1, \text{H}^3) = 1.6$  Hz. <sup>c</sup> $^3J(\text{H}^2, \text{H}^3) = 5.3$  Hz,  $^3J(\text{H}^2, \text{H}^1) = 1.9$  Hz. <sup>d</sup> $^3J(\text{H}^3, \text{H}^2) = 5.3$  Hz,  $^4J(\text{H}^3, \text{H}^1) = 1.6$  Hz,  $^4J(\text{H}^3, \text{H}^4) = 0.7$  Hz. <sup>e</sup>Assignment to  $\text{H}^\alpha$  confirmed by NOE and/or 2D  $^{13}\text{C}$ - $^1\text{H}$  HETCOR experiments.

meters for **6a** and **6b** differ only slightly in the solid state (vide supra).

### 3. Experimental

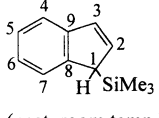
#### 3.1. General

The syntheses were carried out in Schlenk vessels under purified Ar, using carefully dried and oxygen-free solutions. The solvents were dried under reflux ( $\text{C}_6\text{H}_{14}$  over Na/K alloy, THF over  $\text{LiAlH}_4$  and  $\text{CH}_2\text{Cl}_2$  over  $\text{P}_4\text{O}_{10}$ ) and distilled before use in a stream of Ar.

#### 3.1.1. Instrumentation

$^1\text{H}$ -,  $^{13}\text{C}$ - and  $^{29}\text{Si}$ -NMR spectroscopy: Bruker ARX 250 ( $\text{CDCl}_3$  solutions); typical mixing times for NOE experiments [28] were 0.8–1.2 s; 2D  $^{13}\text{C}$ - $^1\text{H}$  HETCOR experiments were based on  $^1J(^{13}\text{C}, ^1\text{H}) = 180$  Hz, using the BIRD pulse for suppression of non-geminal  $^1\text{H}$ - $^1\text{H}$  coupling [29];  $^{29}\text{Si}$ -NMR spectra were recorded by using refocused INEPT experiments with  $^1\text{H}$  decoupling [30]. Mass spectrometry: Finnigan MAT 8500 (EI-MS). X-ray crystallography: Siemens P4 Four-Circle-Diffractometer (**3b**, **4b** and **6b**), STOE IPDS (**6a**); Mo-K $_{\alpha}$  radiation ( $\lambda = 71.073$  pm) with graphite monochromator; crystals were sealed under Ar in Lindemann capillaries. The crystal data and experimental details of the structure determination are given in Table 8.

Table 7  
 $^{13}\text{C}$ -NMR data of the indenyl complexes **1a**, **5a** and **6a** in  $\text{CDCl}_3$

No. Complex	Ferrocene					Indenyl								
	Cp	$\text{C}^1$	$\text{C}^\alpha$	$\text{C}^\beta$	$\text{CH}_3(\text{Si})$	$\text{C}^1$	$\text{C}^2$	$\text{C}^3$	$\text{C}^4$	$\text{C}^5$	$\text{C}^6$	$\text{C}^7$	$\text{C}^8$	$\text{C}^9$
 (neat, room temp.) [27]					-2.2	46.8	135.5	129.4	121.4	125.2	124.1	122.9	145.6	144.5
<b>1a</b> Fc-SiMe <sub>2</sub> (ind)	68.2	69.0	73.5	71.1	-3.9	47.2	135.8	128.7	120.8	124.6	123.3	122.9	144.8	144.0
			73.1	70.9	-4.5									
<b>5a</b> fc[SiMe <sub>2</sub> (ind)] <sub>2</sub>		69.5	73.7	71.6	-3.91/-3.86	47.2	135.7	128.9	120.8	124.7	123.4	123.0	144.9	144.1
			73.2	71.4	-4.51/-4.46									
<b>6a</b> fc[SiMe(ind)]		32.9	75.2 <sup>a</sup>	77.71	-9.4	42.3	133.4	130.7	121.5	125.5	124.2	123.6	144.4/144.3	
		32.3	75.1	77.68										

<sup>a</sup>Assignment to  $\text{C}^\alpha$  confirmed by NOE and 2D  $^{13}\text{C}$ - $^1\text{H}$  HETCOR experiments.

Table 8  
Crystal data and experimental details of the structure determinations<sup>a</sup>

Complex	<b>3b</b>	<b>4b</b> <sup>b</sup>	<b>6a</b>	<b>6b</b>
Formula	C <sub>38</sub> H <sub>32</sub> FeSi	C <sub>36</sub> H <sub>27</sub> ClFeSi	C <sub>20</sub> H <sub>17</sub> FeSi	C <sub>24</sub> H <sub>20</sub> FeSi
Molecular mass	643.48	578.97	341.28	392.34
Diffractometer	Siemens P4	Siemens P4	STOE IPDS	Siemens P4
Temperature (K)	293(2)	296(2)	293(2)	293(2)
Wave length (Å)	0.71073	0.71073	0.71073	0.71073
Crystal system	Triclinic	Triclinic	Orthorhombic	Monoclinic
Space group	<i>P</i> $\bar{1}$	<i>P</i> $\bar{1}$	<i>Pbca</i>	<i>P</i> 2 <sub>1</sub> / <i>c</i>
Unit cell dimensions				
<i>a</i> (Å)	10.6640(12)	9.9345(14)	19.350(4)	7.943(2)
<i>b</i> (Å)	12.2043(11)	10.6423(17)	7.6250(15)	13.192(3)
<i>c</i> (Å)	14.1828(19)	13.4753(14)	21.579(4)	18.230(6)
$\alpha$ (°)	65.448(7)	77.240(9)		
$\beta$ (°)	70.113(9)	84.402(9)		101.87(2)
$\gamma$ (°)	77.647(7)	82.753(10)		
<i>V</i> (Å <sup>3</sup> )	1573.1(3)	1374.8(3)	3183.9(11)	1869.4(9)
<i>Z</i>	2	2	8	4
<i>D</i> <sub>calc</sub> (g cm <sup>-3</sup> )	1.358	1.339	1.424	1.394
Absorption coefficient (mm <sup>-1</sup> )	0.714	0.714	1.015	0.875
Crystal size (mm)	0.18 × 0.14 × 0.12	0.25 × 0.18 × 0.12	0.20 × 0.16 × 0.06	0.25 × 0.16 × 0.12
Theta range (θ)	1.65–24.99	1.97 to 27.50	2.16 to 28.08	1.92 to 25.00
Index ranges	–1 ≤ <i>h</i> ≤ 12, –13 ≤ <i>k</i> ≤ 13, –16 ≤ <i>l</i> ≤ 16	–12 ≤ <i>h</i> ≤ 1, –13 ≤ <i>k</i> ≤ 13, –17 ≤ <i>l</i> ≤ 17	–25 ≤ <i>h</i> ≤ 25, –10 ≤ <i>k</i> ≤ 9, –28 ≤ <i>l</i> ≤ 28	–9 ≤ <i>h</i> ≤ 1, –1 ≤ <i>k</i> ≤ 15, –21 ≤ <i>l</i> ≤ 21
Reflections observed	6309	7314	28065	4389
Independent reflections	5371	6238	3848	3266
<i>R</i> <sub>int</sub>	0.0271	0.0583	0.1259	0.0692
Absorption correction	Empirical ( $\psi$ -scans)	Empirical ( $\psi$ -scans)	Numerical	Empirical ( $\psi$ -scans)
Max/min transmission	0.4657/0.3781	0.4124/0.3667	-	0.4466/0.3254
<i>R</i> [ <i>I</i> > 2σ( <i>I</i> )]	<i>R</i> <sub>1</sub> = 0.0618	<i>R</i> <sub>1</sub> = 0.0440	<i>R</i> <sub>1</sub> = 0.0471	<i>R</i> <sub>1</sub> = 0.0622
<i>wR</i> <sub>2</sub>	0.1815	0.0980	0.0985	0.1495

<sup>a</sup> The hydrogen atoms are in calculated positions. All non-hydrogen atoms were refined with anisotropic temperature factors. The hydrogen atoms were refined applying the riding model with fixed isotropic temperature factors.

<sup>b</sup> The elementary cell contains 2 molecules CH<sub>2</sub>Cl<sub>2</sub>.

### 3.2. Synthesis of the educts 1–6

#### 3.2.1. Lithiation of ferrocene (general procedures)

(a) Ferrocene (5.00 g, 26.88 mmol) was dissolved in 30 ml of THF. In the course of 15 min a solution of 26.9 mmol *t*-BuLi (17.9 ml of a 1.5 M C<sub>5</sub>H<sub>12</sub> solution) was added dropwise at 0 °C. Hexane (40 ml) was then added, and the solution was kept at –78 °C for 15 min, before the orange precipitate was filtered off, washed with small portions of C<sub>6</sub>H<sub>14</sub> and dried in a high vacuum (10<sup>-2</sup> mbar). Yield: 4.50 g (87.2%) FcLi.

(b) Ferrocene (5.00 g, 26.88 mmol) was dissolved in 100 ml of C<sub>6</sub>H<sub>14</sub>. A solution containing 9.2 ml (60 mmol) tetramethylethylenediamine (tmeda) and 35 ml (56 mmol) of a 1.6 M C<sub>6</sub>H<sub>14</sub> solution of *n*-BuLi in 30 ml of C<sub>6</sub>H<sub>14</sub> was then dropwise added, and the reaction mixture was stirred over night. The orange precipitate of fcli<sub>2</sub> (tmeda) was collected and directly used for further reactions.

#### 3.2.2. Preparation of the chlorosilyl-ferrocene educts

3.2.2.1. Chlorodimethylsilyl-ferrocene, Fc–SiMe<sub>2</sub>Cl (**1**). A THF solution (20 ml) containing 0.67 g (3.5 mmol) FcLi was dropwise added to a THF solution (10 ml) of 1.67 ml (13.9 mmol) SiMe<sub>2</sub>Cl<sub>2</sub> at –30 °C. The combined solutions were kept for 30 min at –30 °C and then stirred over night at room temperature (r.t.). The solvent THF was evaporated together with the excess of SiMe<sub>2</sub>Cl<sub>2</sub> under vacuum, the orange residue dissolved in C<sub>6</sub>H<sub>14</sub> (30 ml) and the solution filtered over Na<sub>2</sub>SO<sub>4</sub>. The solvent C<sub>6</sub>H<sub>14</sub> was removed under vacuum and the product heated to 50 °C under high vacuum for 1 h in order to sublime the impurities of ferrocene off. The remaining dark-orange oil (yield 0.69 g, 70.75%) can be used directly for further reactions (cf. [7], yield 78%, b.p. 98–100 °C/0.5 mmHg).

The educts **2–4** were obtained in an analogous manner.



### 3.2.3. Chloromethylphenylsilyl-ferrocene, $Fc-SiMe(Ph)Cl$ (**2**)

Starting from 1.20 g (6.25 mmol)  $FcLi$ , dissolved in 50 ml of THF, and 4.0 ml (25 mmol)  $SiMe(Ph)Cl_2$  in 20 ml of THF, a crop of 1.43 g (67%) yellow crystals was obtained by crystallisation from a concd.  $C_6H_{14}$  solution at  $-80$  °C.

### 3.2.4. Dichloromethylsilyl-ferrocene, $Fc-SiMeCl_2$ (**3**)

The reaction of a THF solution (20 ml) containing 1.40 g (7.29 mmol)  $FcLi$  with another THF solution (10 ml) containing 3.4 ml (29 mmol)  $SiMeCl_3$  gave, after workup, 1.50 g (68.8%)  $Fc-SiMeCl_2$  as a dark-orange oil (cf. [9], 23%, dark-red crystalline solid, b.p.  $130$  °C/0.05 mmHg).

### 3.2.5. Trichlorosilyl-ferrocene, $Fc-SiCl_3$ (**4**)

A solution of 2.60 g (13.54 mmol)  $FcLi$  in dimethoxyethane (DME, 10 ml) was added dropwise to 7.0 ml (61 mmol)  $SiCl_4$ , and the reaction mixture was stirred over night. The solvent was evaporated and the residue dissolved in 30 ml of  $C_5H_{12}$ . The  $C_5H_{12}$  solution was filtered over  $Na_2SO_4$ , brought to dryness and the residue heated to  $50$  °C under high vacuum. Yellow powder of  $Fc-SiCl_3$ , yield 2.7 g (64.3%) (cf. [10], yield 25% after vacuum sublimation, m.p.  $75-77$  °C).

### 3.2.6. 1,1'-Bis[chloromethylsilyl]ferrocene, $fc[SiMe_2Cl]_2$ (**5**)

A suspension of 8.44 g (26.87 mmol)  $fcLi_2(tmeda)$  in  $C_6H_{14}$  (100 ml) was added dropwise to a  $C_6H_{14}$  solution (40 ml) of 12.9 ml (107.4 mmol)  $SiMe_2Cl_2$ . The reaction mixture was stirred for 4 h. The volatile components (including  $SiMe_2Cl_2$  and  $tmeda$ ) were removed under high vacuum. The residue was redissolved in  $C_6H_{14}$ , and the solution was filtered over  $Na_2SO_4$ . The orange-red solution was concentrated to ca. 20 ml and cooled to  $-80$  °C over night. Orange crystals of  $fc[SiMe_2Cl]_2$ , yield 5.40 g (54.1%) (cf. [11], yellow-orange solid, m.p.  $89$  °C).

### 3.2.7. 1-Chloromethylsila-[1]ferrocenophane, $fc[SiMeCl]$ (**6**)

A  $C_6H_{14}$  solution (100 ml) of 3.4 ml (29 mmol)  $SiMeCl_3$  was slowly added at  $-78$  °C to the educt  $fcLi_2(tmeda)$  which had been prepared from 5.00 g (26.88 mmol) ferrocene (see above). The reaction mixture was stirred over night, then brought to dryness and the residue redissolved in  $C_6H_{14}$ . Filtration over  $Na_2SO_4$  and concentration to ca. 20 ml gave an orange-red  $C_6H_{14}$  solution. Upon cooling to  $-80$  °C, orange-red crystals of  $fc[SiMeCl]$  were obtained, yield 5.95 g (84.3%) (cf. [12][13], yield 88%).

## 3.3. Synthesis of the indenyl- and fluorenyl-substituted silanes

### 3.3.1. General procedure

About 3 mmol of the chlorosilyl educt (**1-6**) are dissolved in 20–50 ml of THF, and a THF solution (40–50 ml) containing a slight excess (5–15%) of the respective stoichiometric amount of either indenyl- or fluorenyl-lithium is slowly added at  $-30$  °C. The solution is stirred at r.t. for 20 h (over night). The solvent THF is then evaporated in a high vacuum ( $10^{-2}$  mbar) and the residue redissolved in  $C_6H_{14}$ ,  $CH_2Cl_2$  or mixtures of these solvents. After filtration over  $Na_2SO_4$ , the solutions were cooled to  $-80$  °C to give crystalline products in nearly all cases.

### 3.3.2. $Fc-SiMe_2(ind)$ (**1a**)

Starting from 1.10 g (3.9 mmol) **1** and 0.50 g (4.10 mmol) indenyl-lithium, a dark-orange oil was obtained (1.07 g, 76.6%) which could not be crystallised. EI-MS:  $m/e = 358$  [ $M^+$ , 77%], 234 ( $Fc-SiMe_2^+$ , 100%).

### 3.3.3. $Fc-SiMe_2(flu)$ (**1b**)

Crystallisation from  $C_6H_{14}$  gave 0.54 g (73.5%) yellow-orange crystals, m.p.  $70-72$  °C. EI-MS:  $m/e = 408$  [ $M^+$ , 73%], 243 ( $Fc-SiMe_2^+$ , 100%).

### 3.3.4. $Fc-SiMe(Ph)(flu)$ (**2b**)

The reaction of 0.33 g (0.97 mmol) **2** with 0.17 g (0.99 mmol) fluorenyl-lithium gave, after crystallisation from  $C_6H_{14}-CH_2Cl_2$  (1:4) orange crystals, m.p.  $75-77$  °C, yield 0.37 g (81%). EI-MS:  $m/e = 470$  [ $M^+$ , 92%], 305 ( $Fc-SiMePh^+$ , 100%).

### 3.3.5. $Fc-SiMe(flu)_2$ (**3b**)

Yellow crystals (from  $C_6H_{14}$ ), m.p.  $78-81$  °C, yield 0.55 g (50%). EI-MS:  $m/e = 558$  [ $M^+$ , 27%], 393 ( $Fc-SiMe(flu)^+$ , 100%).

### 3.3.6. $Fc-SiCl(flu)_2$ (**4b**)

The reaction of 0.27 g (0.82 mmol) **4** with 0.31 g (1.80 mmol) fluorenyl-lithium (in 80 ml THF) produced, after crystallisation from  $CH_2Cl_2$ , yellow crystals (0.27 g (56.9%), m.p.  $219$  °C (dec.). EI-MS:  $m/e = 578$  [ $M^+$ , 65%], 413 ( $Fc-SiCl(flu)^+$ , 100%).

### 3.3.7. $fc[SiMe_2(ind)]_2$ (**5a**)

Orange oil, yield 0.30 g (47%). EI-MS:  $m/e = 530$  [ $M^+$ , 81%], 415 ( $fc(SiMe_2)_2(ind)^+$ , 100%), 300 ( $fc(SiMe_2)_2^+$ , 62%).

### 3.3.8. $fc[SiMe_2(flu)]_2$ (**5b**)

Yellow crystals from  $C_6H_{14}-CH_2Cl_2$  (1:2), m.p.  $204-206$  °C, yield 75%. EI-MS:  $m/e = 630$  [ $M^+$ , 65%], 465 ( $fc(SiMe_2)_2(flu)^+$ , 100%), 300 ( $fc(SiMe_2)_2^+$ , 12%).

### 3.3.9. *fc[SiMe(ind)]* (**6a**)

The reaction of 0.66 g (2.51 mmol) **6** with 0.34 g (2.78 mmol) indenyl-lithium in 70 ml of THF gave, upon crystallisation from C<sub>6</sub>H<sub>14</sub>–CH<sub>2</sub>Cl<sub>2</sub> (2:1), 0.57 g (66%) red crystals, m.p. 149–153 °C. EI-MS: *m/e* = 342 [M<sup>+</sup>, 100%], 227 (fc[SiMe]<sup>+</sup>, 69%).

### 3.3.10. *fc[SiMe(flu)]* (**6b**)

Yellow–orange crystals (from CH<sub>2</sub>Cl<sub>2</sub>), m.p. 142–145 °C, yield 66%. EI-MS: *m/e* = 392 [M<sup>+</sup>, 100%], 227 (fc[SiMe]<sup>+</sup>, 100%).

## 4. Supplementary information

Crystallographic data (excluding structure factors) for the structures reported in this paper have been deposited with the Cambridge Crystallographic Data Centre, CCDC nos. 186753 (**3b**), 186754 (**4b**), 186755 (**6a**) and 186752 (**6b**). Copies of this information may be obtained free of charge from the Director, CCDC, 12 Union Road, Cambridge CB2 1EZ, UK [Fax: +44-1223-336033; e-mail: deposit@ccdc.cam.ac.uk or www: <http://www.ccdc.cam.ac.uk>].

## Acknowledgements

Support of this work by the Deutsche Forschungsgemeinschaft, the Deutsche Akademische Austauschdienst (DAAD) and the Fonds der Chemischen Industrie is gratefully acknowledged.

## References

- [1] P. Escarpa Gaede, *J. Organomet. Chem.* 616 (2000) 29.
- [2] H.G. Alt, R. Zenk, *J. Organomet. Chem.* 512 (1996) 51.
- [3] R. Broussier, M. Laly, P. Perron, B. Gautheron, S. M'Koyan, P. Kalck, N. Wheatley, *J. Organomet. Chem.* 574 (1999) 267.
- [4] cf. M. Herberhold, Y.-X. Cheng, G.-X. Jin, W. Milius, *Z. Naturforsch. Teil B* 55 (2000) 814.
- [5] F. Rebiere, O. Samuel, H.B. Kagan, *Tetrahedron Lett.* 31 (1990) 3121.
- [6] M.D. Rausch, D.J. Ciappenelli, *J. Organomet. Chem.* 10 (1967) 127.
- [7] K.H. Pannell, H. Sharma, *Organometallics* 10 (1991) 954.
- [8] M.D. Rausch, G.C. Schloemer, *Org. Prep. Proced.* 1 (1969) 131.
- [9] D. Foucher, R. Ziembinski, R. Petersen, J. Pudelski, M. Edwards, Y. Ni, J. Massey, C.R. Jaeger, G.J. Vancso, I. Manners, *Macromolecules* 27 (1994) 3992.
- [10] M.S. Wrighton, M.C. Palazzotto, A.B. Bocarsly, J.M. Bolts, A.B. Fischer, L. Nadjó, *J. Am. Chem. Soc.* 100 (1978) 7264.
- [11] D.L. Zechel, D.A. Foucher, J.K. Pudelski, G.P.A. Yap, A.L. Rheingold, I. Manners, *J. Chem. Soc. Dalton Trans.* (1995) 1893.
- [12] A. Spannenberg, P. Arndt, M. Oberthür, R. Kempe, *Z. Anorg. Allg. Chem.* 623 (1997) 389.
- [13] D.L. Zechel, K.C. Hultzsch, R. Rulkens, D. Balaisish, Y. Ni, J.K. Pudelski, A.J. Lough, I. Manners, *Organometallics* 15 (1996) 1972.
- [14] L. Silaghi-Dumitrescu, I. Haiduc, R. Cea-Olivares, I. Silaghi-Dumitrescu, J. Escudié, C. Couret, *J. Organomet. Chem.* 545–546 (1997) 1.
- [15] M.J. MacLachlan, A.J. Lough, W.E. Geiger, I. Manners, *Organometallics* 17 (1998) 1873.
- [16] M.J. MacLachlan, M. Ginzburg, J. Zheng, O. Knöll, A.J. Lough, I. Manners, *New J. Chem.* (1998) 1409.
- [17] V.V. Deméteev, F. Cervantes-Lee, L. Parkányi, H. Sharma, K.H. Pannell, M.T. Nguyen, P. Diaz, *Organometallics* 12 (1993) 1983.
- [18] M. Herberhold, *Angew. Chem.* 107 (1985) 1985; M. Herberhold, *Angew. Chem. Int. Ed. Engl.* 34 (1985) 1837.
- [19] (a) K.H. Pannell, V.V. Dementiev, H. Li, F. Cervantes-Lee, M.T. Nguyen, A.F. Diaz, *Organometallics* 13 (1994) 3644; (b) M.Y. Antipin, I.I. Vorontsov, I.I. Dubovik, V. Papkov, F. Cervantes-Lee, K.H. Pannell, *Can. J. Chem.* 78 (2000) 1511.
- [20] W. Finckh, B. Tang, D.A. Foucher, D.B. Zambie, R. Ziembinski, A. Lough, I. Manners, *Organometallics* 12 (1993) 823.
- [21] (a) H. Stoeckli-Evans, A.G. Osborne, R.H. Whiteley, *Helv. Chim. Acta* 59 (1976) 2402; (b) cf. H. Stoeckli-Evans, A.G. Osborne, R.H. Whiteley, *J. Organomet. Chem.* 194 (1980) 91.
- [22] F.H. Köhler, W.A. Geike, N. Hertkorn, *J. Organomet. Chem.* 334 (1987) 359.
- [23] M. Herberhold, W. Milius, U. Steffl, K. Vitzithum, B. Wrackmeyer, R.H. Herber, M. Fontani, P. Zanello, *Eur. J. Inorg. Chem.* (1999) 145.
- [24] (a) H. Marsmann, in: R. Diehl, E. Fluck, R. Kosfeld (Eds.), *NMR—Basic Principles and Progress*, vol. 17, Springer, Berlin, 1981, p. 65; (b) E. Kupce, E. Lukevics, in: E. Buncl, J.R. Jones (Eds.), *Isotopes in the Physical and Biomedical Sciences*, vol. 2, Elsevier, Amsterdam, 1991, pp. 213–295.
- [25] E. Pretsch, J. Seibl, W. Simon, Th. Clerc, *Tabellen zur Struktur- aufklärung organischer Verbindungen mit spektroskopischen Methoden*, 3rd ed., Springer-Verlag, Berlin, New York, Heidelberg, 1990.
- [26] (a) I.V. Borisova, N.N. Zemlyanskii, Yu.N. Luzikov, Yu.A. Ustynuk, V.K. Belskii, N.D. Kolosova, M.M. Shtern, I.P. Béletskaya, *Dokl. Akad. Nauk SSSR* 269 (1983) 369; (b) I.V. Borisova, N.N. Zemlyanskii, Yu.N. Luzikov, Yu.A. Ustynuk, V.K. Belskii, N.D. Kolosova, M.M. Shtern, I.P. Béletskaya, *Chem. Abstr.* 99 (1983) 105383.
- [27] Yu.N. Luzikov, N.M. Sergeev, Yu.A. Ustynuk, *J. Organomet. Chem.* 65 (1974) 303.
- [28] (a) G. Bodenhausen, H. Kogler, R.R. Ernst, *J. Magn. Reson.* 58 (1984) 370; (b) G. Wider, S. Macura, A. Kumar, R.R. Ernst, K. Wüthrich, *J. Magn. Reson.* 56 (1984) 207.
- [29] (a) J.R. Garbow, D.P. Weitekamp, A. Pines, *Chem. Phys. Lett.* 93 (1982) 504; (b) V. Rutar, *Chem. Phys. Lett.* 106 (1984) 258.
- [30] (a) G.A. Morris, R. Freeman, *J. Am. Chem. Soc.* 101 (1979) 760; (b) G.A. Morris, *J. Am. Chem. Soc.* 102 (1980) 428; (c) D.P. Burum, R.R. Ernst, *J. Magn. Reson.* 39 (1980) 163.
- [31] S.-G. Lee, S.S. Lee, Y.K. Chung, *Inorg. Chim. Acta* 286 (1999) 215.